ILASS Americas, 22nd Annual Conference on Liquid Atomization and Spray Systems, Cincinnati, OH, May 2010

Experimental and Computational Study of a Spray at Multiple Injection Angles Impact Study of a Clean in Place Tank Wash System

K. J. Brown*, W. Kalata and R. J. Schick
Spray Analysis and Research Services
Spraying Systems Co.
Wheaton, IL 60187 USA

M. Sami, A. Maruszewski and A. Parihar
ANSYS Inc.
Evanston, IL 60201 USA

Abstract

Selecting and optimizing a clean in place (CIP) system for tank wash applications is a complex process. Automated tank cleaning systems can result in thousands of dollars in savings due to reduced production downtime costs and labor costs. One of the parameters in an effective cleaning system is impact. Due to the dynamic nature of CIP systems and endless variations in tank dimensions, wall impact has been an elusive metric.

A case study has been performed to examine wall impact for a typical CIP system. In the current study, a stainless steel tank with a 66inch diameter was selected. A motor driven, solid stream nozzle was used at moderate pressures for the empirical study. Static impact and dynamic impact were acquired using pressure sensitive detector techniques. The baseline static impact measurements in the present study were obtained at various distances and operating conditions under laboratory conditions. The dynamic impact measurements were obtained with the air actuated nozzle inside of a stainless steel tank at multiple locations. Comparisons of static impact and dynamic impact were assessed. A computational fluid dynamics (CFD) model was performed to address the wide dimensional variations in vessels. The spray simulations of the rotating nozzle system were conducted using ANSYS FLUENT computational fluid dynamics (CFD) package. Congruence between the model and empirical data was determined.

*Corresponding author

Introduction

Selecting and optimizing a clean in place (CIP) system for tank wash applications is a complex process Effective cleaning and sanitizing is important in controlling the transmission of diseases and improves the shelf life and sensory quality of food products.

In a collision, the change in momentum that a body undergoes is equal to the collision force times the duration of the collision.

$$\Delta(mv) = F\Delta t = \int F(t)dt \qquad (1)$$

Similarly, when a water jet impinges on a solid plate, an initial pressure occurs which is comparable to the water-hammer pressure of Cook.[1]

$$P = \rho \upsilon c \qquad (2)$$

The initial high pressure given by equation 2, decays very rapidly due to release waves propagating into the jet from its circumference followed by lateral jetting. Once steady state is reached, the pressure approaches the hydrodynamical pressure.

$$P = \frac{1}{2} \rho \upsilon^2 \qquad (3)$$

This impact pressure is used to remove residual soils and chemicals from the interior of tanks. There are several factors that affect impact pressure and cleaning effectiveness, such as: type of residue, cleaning chemicals used, water temperature, flow rate, pressure, spray pattern, spray angle (relative to substrate), spray distance and rotational velocity of the water jet.

For this study, the scope was focused on the impact pressure as it is closely related to cleaning effectiveness while removing some design parameters. This reduces the design space to a manageable quantity.

Process improvement and optimization in the vessel cleaning industry is a constantly ongoing effort. The improvements made in nozzle design and liquid atomization in recent years have provided the possibility of process optimization like never before. While on-site experimental testing provides the most direct assessment of a spray's characteristics, often the cost and availability of testing is limited. Therefore, computational fluid dynamics (CFD) projects for this type of application have become very useful. Using CFD methods, process engineers are able to, for the first time, assess the spray quality within the *actual* spray process region. The increased use of CFD to model these processes requires in-depth validation of the methods used to model these applications and the results provided by these types of models.

Spraying Systems Co. has the unique combination of testing and modeling expertise which allow for a rigorous validation of these modeling techniques often used to simulate *un-testable* situations.

Equipment and Methods

Experimental Setup and Methods

The empirical setup consisted of a spray nozzle, impact measurement device, a static test plate and a stainless steel vessel. All tests were carried out with spray liquid (water) at ambient temperature, ~68°F. The nozzle was operated with a steady 3.8 bar (55psi) clean water supply for all tests.

Nozzle Information

An AA190 tank wash lance with dual 0030 solid stream nozzles was selected based on tank geometry. The lance provides a total flow of .826kg/sec, split evenly between the two outlets. The orifices rotate about two axis, as shown in Figure 1.

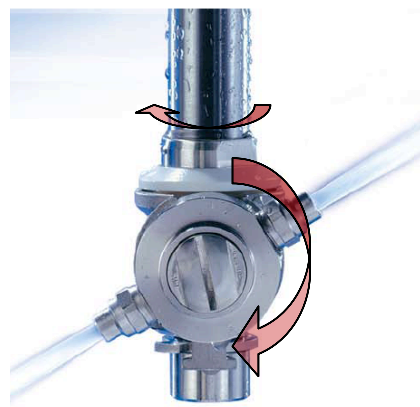

Figure 1. AA190 lance with rotation noted.

Various operating conditions were modified to examine the effects on impact pressure. Spray distance, rotations speed, flow rate and impact angle were examined through the range of: 0.305 – 0.914m, 1-8rpm, .2-.5kg/s, and 0-30° respectively. Initial testing was performed inside of a 550gal, ∅ 1.524m, stainless steel tank to simulate a clean in place (CIP) environment. Due to the complexities of data acquisition in the tank, the majority of impact testing was carried out in a laboratory setting to simulate process conditions. Figure 2, provides an image of the setup and clarifies the coordinate system definitions for x, y, z, and α. The z-direction axis runs parallel to the nozzle direction; negative y indicates the direction of gravitational pull and is held normal to the impact measurement pad.

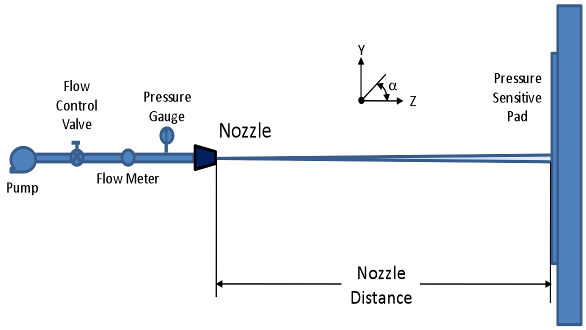

Figure 2. Empirical Setup.

Impact Measurement

A pressure sensitive pad was used for acquisition of impact data. The pad was 0.152m x 0.152m in size with 256 measurement points within the pad area. Data is acquired in real time with a 0.25 frames/sec speed. The pressure pad was affixed to a stationary plate that was initially arranged normal to the nozzle direction. Distances from nozzle tip to the pad surface were recorded throughout the trials. The impact was acquired both statically (with no rotation) and dynamically (with rotation controlled by air actuation). Figure 3-4 provides pictorial evidence of the empirical setup and the software used for impact measurement, respectively.

Figure 3. Empirical Setup.

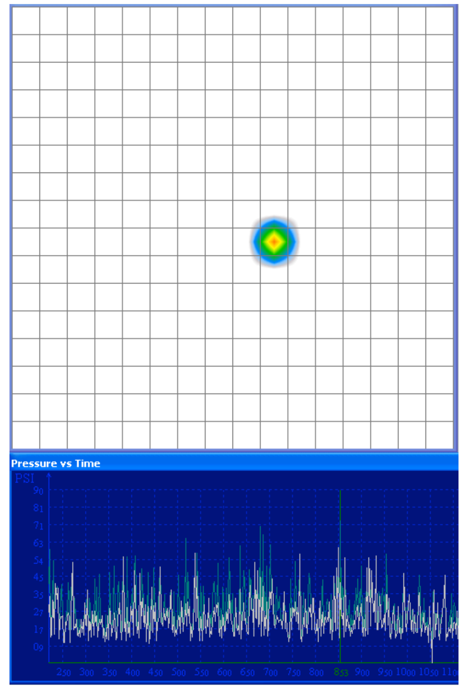

Figure 4. Impact Pressure Software

Computational Methods

CFD simulations were performed with ANSYS FLUENT version 12.1. Generally, the CFD model was reproduced according to the wind tunnel geometry including the spray injector which was minimally simplified to reduce the complexity of the computational mesh size. Meshing was performed within GAMBIT 2.4. Dense mesh was incorporated in the near vicinity of the spray injection locations. Size functions were used to further reduce mesh size. The 3D mesh consisted of mixed elements with approximately 1.4 million cells. Figure 5 provides a pictorial description of the tank with figure 6 describing the two-dimensional schematic of the CFD model setup and defines the coordinate system referenced in both the computational and experimental results.

Figure 5. Physical Tank

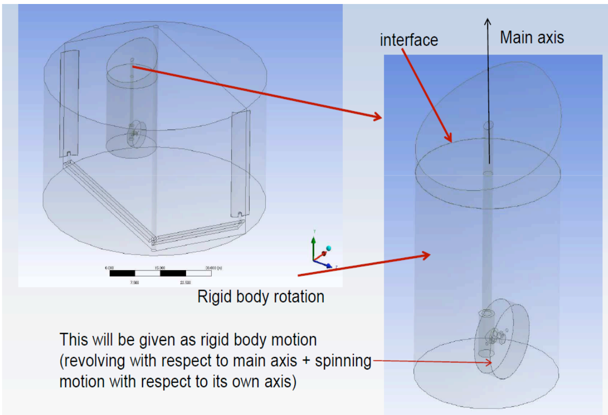

Figure 6. CFD model setup

The CFD model was set up with a mass-flow inlet boundary condition (BC) for the simulation of the liquid jet. A sliding mesh scheme was used to simulate the rotation about both axis to simulate movement of the CIP nozzle. The outlet of the simulation was defined with a constant pressure boundary condition to simulate the drain mechanism at the base of the vessel. The vessel and lance walls were specified as rigid with no-slip and adiabatic conditions. Throughout all simulations the following models were included: k-ε Realizable Turbulence Model, VOF implicit compressive model. The air phase was defined as the primary phase, with the liquid jet (water) defined as the secondary phase.

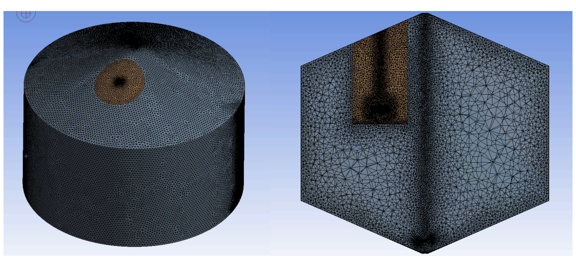

Figure 7. Summary of VOF CFD results.

The initial model was meshed with fine mesh at the injection site and the walls, approximately 4-5 cells across the diameter of the jet inlet. Using size functions the mesh was increased in size moving away from the nozzle and walls. This resulted in a total mesh size of 4.5million. This mesh was determined to be in-valid because the size of the mesh was almost the size of the diameter in places. Since the jet moves through the entire domain, this resolution is not sufficient to capture the physics occurring in the vessel. The mesh was then refined to attain adequate mesh size through the vessel domain. This resulted in the use of more than 50 million cells, which is highly computationally expensive.

Hence forth, the model was split into two parts. The first part is a slice of the vessel using the VOF model. This allows the ability to examine impact of the jet on the wall and the effects of the nozzle rotation.

The velocity profiles for DPM injections were defined via CFD Volume of Fluid (VOF) modeling of the water jet with coupling of the drop size/ velocity pairing to match the momentum of the jet. The DPM simulation was performed in steady state and isothermal condition with constant pressure BC.

Results and Discussion

Empirical Results

The impact results at each position provide an impression of the cleaning effectiveness of the setup. The first characteristic examined was the spray distance. The results were collected at distances from 0.305-0.914m at 0.152m increments at operating pressures. The results of these trials are contained in Figure 8-9. The results follow the expected trends, demonstrating a reduction in impact pressure with an increase in distance to target. The average impact pressure was reduced by 60.5% as the distance was increased through the full range examined for the 689475Pa pressure. The impact pressure was reduced by 32.7% as the distance was increased through the full range of the 1378950Pa trials.

Additionally the area increases slightly with an increase in distance to target. This is due to the turbulence propagation along the injected water jet. The impact area was increased by 36.1% as the distance was increased through the full range examined for the 689475Pa pressure. The impact area was increased by 20.4% as the distance was increased through the full range of the 1378950Pa trials.

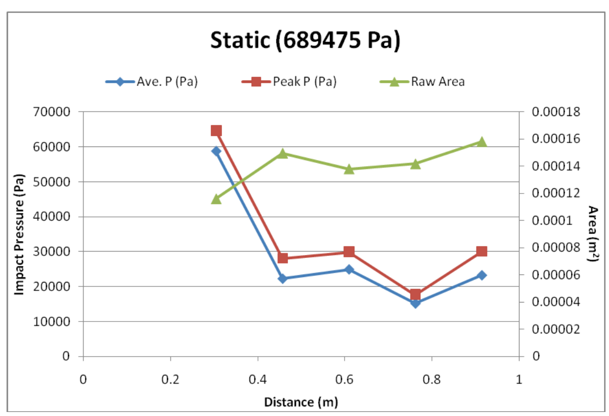

Figure 8. Impact with respect to Distance (LP)

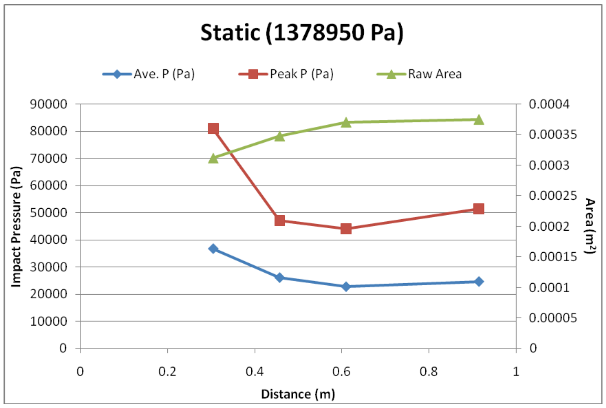

Figure 9. Impact with respect to Distance (HP)

In addition to the effects of distance, these trials evaluated the effects of increased pressure. Average impact pressure varied only slightly. However peak impact pressure was shown to increase by an average of 53.1% (ranging from 25-71%). The increase in impact pressure with an increase in pressure is intuitive. This trend is due to the fact that the exit velocity of liquid is increased providing a greater momentum for impact.

A link between static and dynamic impact was drawn. The dual solid stream nozzles are rotated about two axes, as shown in figure 1. Due to this compound motion, a great deal of momentum is lost. Three rotation speeds were assessed in addition to the static results. The results of these trials are shown in figures 10-11.

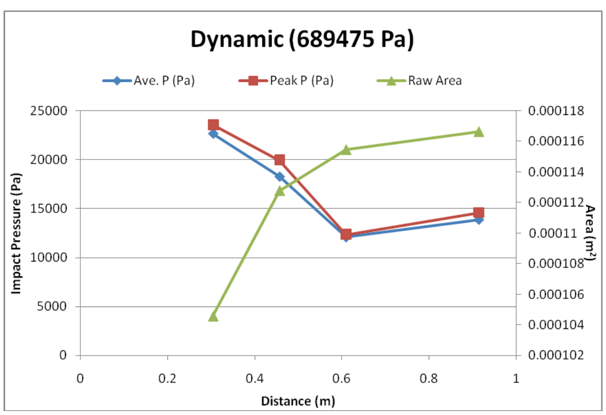

Figure 10. Impact with respect to 8rpm rotation speed.

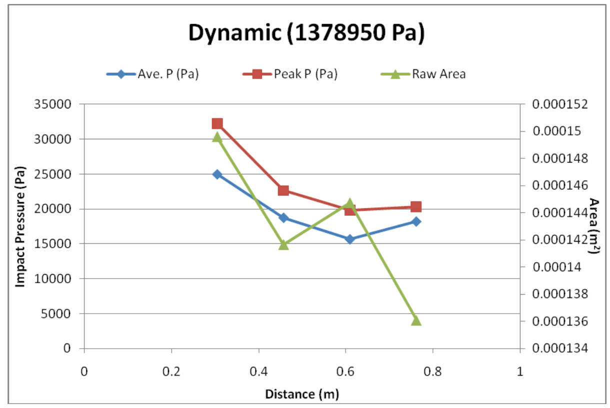

Figure 11. Impact with 8rpm rotation speed.

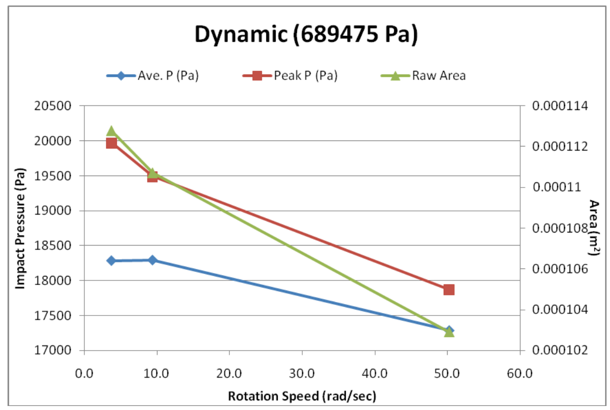

Figure 12. Impact with respect to rotation speed.

Rotational speed significantly reduced the impact pressure. At 689475Pa and a rotational speed of 50.3 rad/sec, the average impact pressure was reduced by an average of 42.7%. The peak impact pressure was reduced by an average of 50.6%. At 1378950, the average impact pressure was reduced by an average of 37.3%. The peak impact pressure was reduced by 60.4%. The losses were fairly consistent throughout the full range of distance, varying less than 10% regardless of spray distance.

To simulate the changing impact angle of the water jet through the rotation of the CIP, three angle were evaluated 0-30°. The results of these trials are shown in figures 13-14.

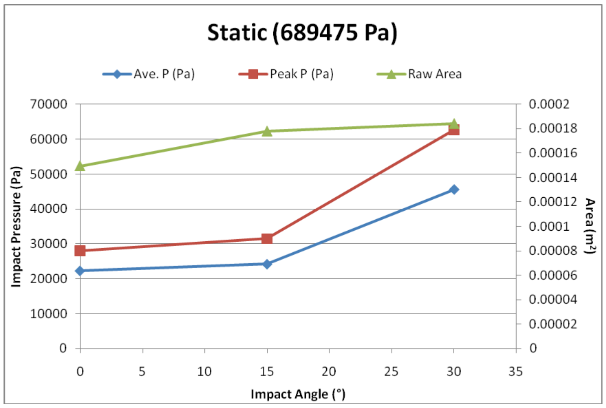

Figure 13. Impact with respect to Impact Angle (LP)

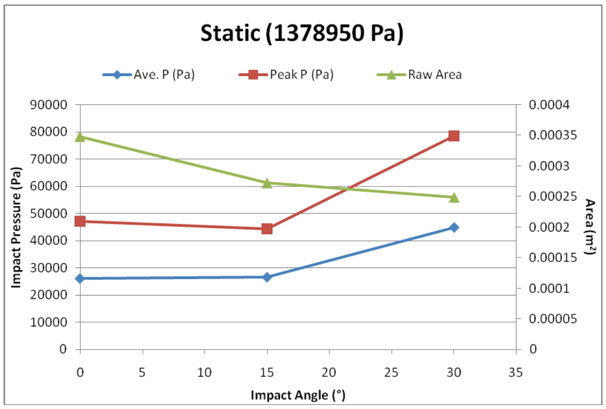

Figure 14. Impact with respect to Impact Angle (HP)

The results of these trials were counterintuitive. Pressure was shown to increase with an increase in impact angle. From 0° to 15° there was a very small increase in impact pressure. From 0° to 30° there was an increase of 66.5% for static measurements, and 46.6% for the dynamic measurements at 1378950Pa. There are a few explanations for this odd phenomenon. The collision of water droplets upon a surface is pretty much inelastic. This would be expected since a water droplet, having a relatively weak surface binding force, is likely to deform and "plane out" in a collision with any solid surface. Figure 15 indicates four possible impact scenarios.

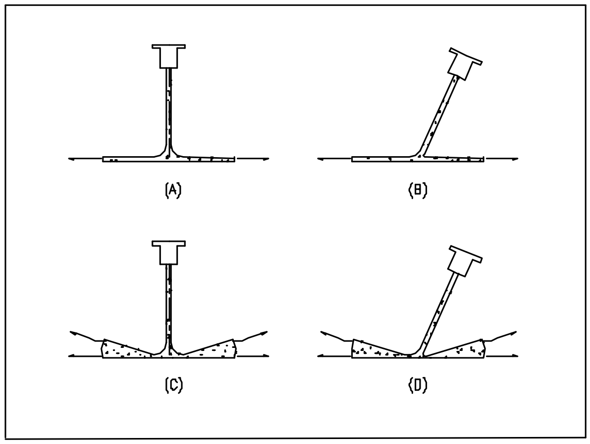

Figure 15. Impact Possibilies

In case A, the spray hits the target surface and deflects horizontally. In case B, the spray strikes at an angle. Cases C and D are similar to A and B, except that the sprays splash upward somewhat. A real situation could be any combination of these situations. Cases A and B would be the type of behavior expected when spraying at lower relative pressures onto smooth surfaces. Cases C and D represent higher pressures, rougher surfaces, and closer target distances, which is the primary reaction occurring in this experiment as reflected in figure 3. Also, the presence of standing liquid could serve to diffuse the spray impact in general. This effect would have the largest impact with a 0º impact angle, due to the fact the liquid will have a greater likelihood to build up at the impact surface. While the larger impact angle will allow the fluid to move smoothly out of the measurement area. While these effects may be interesting, the increased total impact resulting doesn't necessarily help clean the target surface.

CFD Results

The results from the CFD three-dimensional simulations are provided in order of the progression of work. The initial studies were performed to obtain the wall impact at a static, 0° impact angle. The VOF model with simplified geometry was required to obtain this information through CFD. Figure 16 provides some detail of the mesh used to analyze the dual inlet injector.

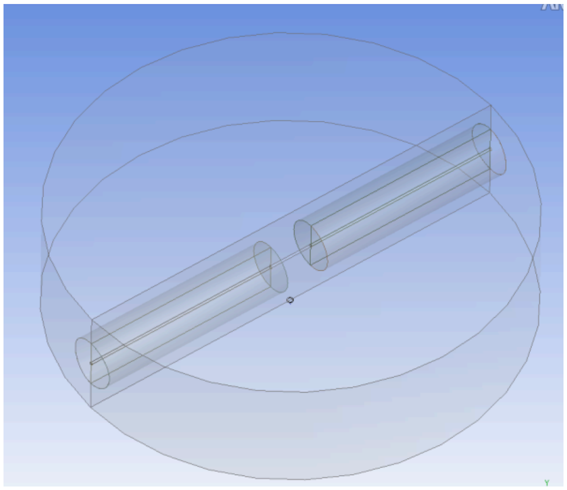

Figure 16. Computational Domain

The model was created using ANSYS Fluent 12.0 solvers in the Workbench environment. The model was created with parametric input to allow for a large deal of variation based on actual tank geometry and actual operating conditions. Computational domain is shown in figure 15. Various nozzle capacities and geometries can be read into the Workbench environment with minimal additional effort. The model employs an automated meshing feature which creates a fine hex mesh in the jet area. Cross-section of resulting mesh is shown in figure 17, below.

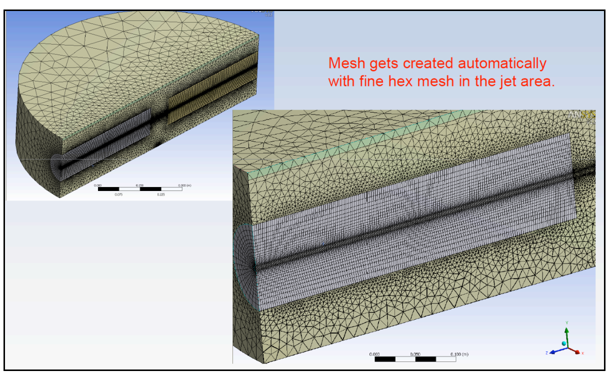

Figure 17. Mesh Details for Jet Analysis

The results indicate a small gravitational drift, with the Jet impacting the opposing wall at a location slightly below the nozzle injection elevation. This effect is verified from pictorial evidence acquired through the empirical trials. A DPM model was used in an attempt to reproduce the jet path using particles. These particles were injected with properties similar to water with particle diameter and velocity which simulates the momentum contained in the jet. By tuning the particle momentum with the water jet, it is possible to predict the jet path using the DPM model. This enables an option to model an entire vessel, to evaluate cleaning cycles, coverage and potential shadowing that may occur in industrial environments. A comparison of these results is shown in Figure 18, below.

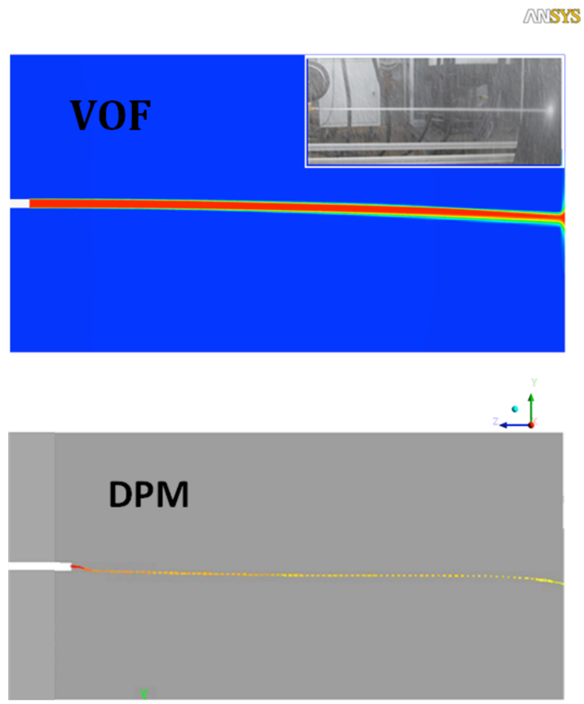

Figure 18. Jet Path

Figure 19 shows the contours of static pressure at the tank wall.

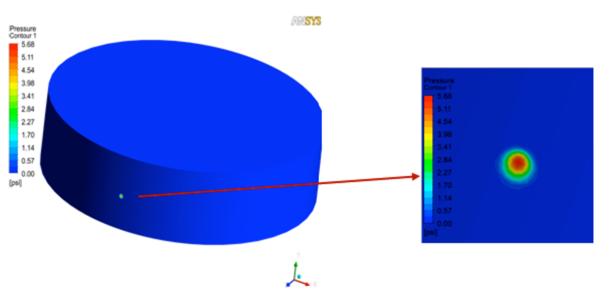

Figure 19. Contours of Static Pressure

An additional VOF model was created with sliding mesh to evaluate the effects of the rotating nozzle relative to the vessel. This model consisted of a 45 degree sector of the tank diameter. The setup is shown in Figure 20, below.

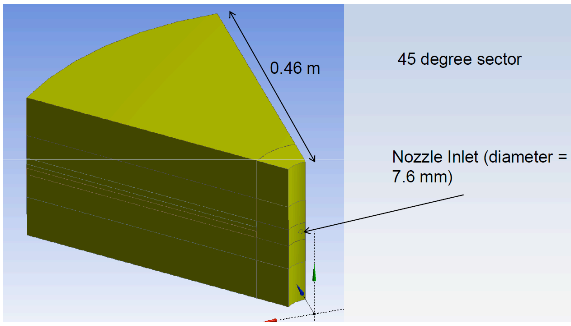

Figure 20. CFD setup (transient).

Again the model was created with parametric input to allow for a large deal of variation based on actual tank geometry and actual operating conditions. Various nozzle capacities and geometries can be read into the Workbench environment with minimal additional effort. The model employs the automated meshing feature of Workbench 12.0, which creates a fine hex mesh in the jet area. The resulting mesh is shown in figure 21, below.

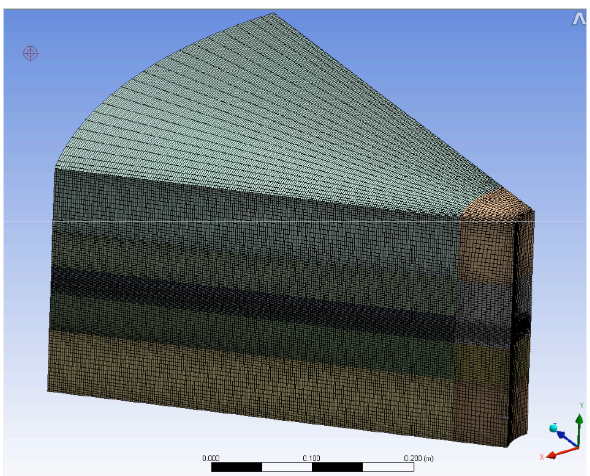

Figure 21. Mesh Details- Hex Mesh Cell ~641,000.

Three models were designed to determine the effects of rotational speed on impact pressure. Run-1 was performed applying a rotational speed of 0 rad/sec, Run-2 was performed with a rotational speed of 0.733rad/sec, and Run-3 utilizes a rotational speed of 3.665 rad/sec. The results of this work is shown in Figure 22.

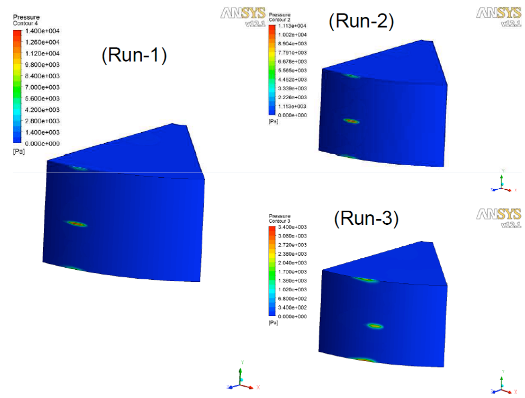

Figure 22. Results (local range).

These trials were run with a 0.413 kg/s inlet mass flow, with air defined as the primary phase and water defined as the secondary phase. An implicit VOF scheme was used, with a time step of 1e-03sec for a total run time of 0.12 sec. An increase in the rotational speed of the nozzle causes a decrease in the average pressure value. This trend is similar to what is observed in the experiments. The simulation predicts a 21% decrease in static pressure value between Run 1 and Run 2; and 72% decrease between Run 2 and Run-3. Empirical data was also found to decrease, however the decline was much steeper for the empirical test data. For experimental conditions similar to Run1 and Run2, a 33% drop in static average pressure was observed compared to the predicted value of 21%.

Conclusions

The experimental and computational results presented herein demonstrate good agreement in the spray characteristics over the broad range of operating conditions. These results demonstrate the validity of computational modeling which may be used in cases were experimental results are unavailable, cost prohibited, or impossible. Future work will include additional CFD and empirical results. Improved input conditions and more rigorous validation of the imposed forces on the vessel are needed to achieve the overall goal of estimating cleaning efficiency of a multitude of CIP systems.

References

1. Bachalo, W.D. and Houser, M.J., "Phase Doppler Spray Analyzer for Simultaneous Measurements of Drop Size and Velocity Distributions," Optical Engineering, Volume 23, Number 5, September-October, 1984.
2. Bachalo, W.D. and Houser, M.J., "Spray Drop Size and Velocity Measurements Using the Phase/Doppler Particle Analyzer", Proceedings of the ICLASS (3rd Intl.), July 1985.

3. Lefebvre, A. H., *Atomization and Sprays*, Hemisphere, New York, 1989.
4. Fluent Inc. FLUENT 12.0 User's Guide, 2010.
5. Brown, K., Kalata, W., Schick, R.J.," Drop Size Distribution Analysis with respect to Height - Numerical Simulation versus Empirical Evaluation", Proceedings of ILASS 2008, May, 2008.